

Dust and star formation in distant radio galaxies

Michiel Reuland,^{1,2,3*} Huub Röttgering,¹ Wil van Breugel,² and Carlos De Breuck⁴

¹*Leiden Observatory, P.O. Box 9513, 2300 RA Leiden, The Netherlands*

²*Institute of Geophysics and Planetary Physics, L-413 Lawrence Livermore National Laboratory, Livermore, CA 94550, USA*

³*Department of Physics, UC Davis, 1 Shields Avenue, Davis, CA 95616, U.S.A.*

⁴*Institut d'Astrophysique de Paris, CNRS, 98bis Boulevard Arago, F-75014 Paris, France*

Accepted XXXX December XX. Received XXXX December XX; in original form XXXX December XX

ABSTRACT

We present the results of an observing program with the SCUBA bolometer array to measure the submillimetre (submm) dust continuum emission of 24 distant ($z > 1$) radio galaxies. We detected submm emission in 12 galaxies with $S/N > 3$, including 9 detections at $z > 3$. When added to previous published results these data almost triple the number of radio galaxies with $z > 3$ detected in the submm and yield a sample of 69 observed radio galaxies over the redshift range $z = 1$ –5. We find that the range in rest-frame far-infrared luminosities is about a factor of 10. We have investigated the origin of this dispersion, correlating the luminosities with radio source power, size, spectral index, K -band magnitude and $\text{Ly}\alpha$ luminosity. No strong correlations are apparent in the combined data set. We confirm and strengthen the result from previous submm observations of radio galaxies that the detection rate is a strong function of redshift. We compare the redshift dependence of the submm properties of radio galaxies with those of quasars and find that for both classes of objects the observed submm flux density increases with redshift to $z \approx 4$, beyond which, for the galaxies, we find tentative evidence for a decline. We find evidence for an anti-correlation between submm luminosity and UV polarisation fraction, for a subsample of 13 radio galaxies, indicating that starbursts are the dominant source of heating for dust in radio galaxies.

Key words: galaxies: active – galaxies: formation – galaxies: high-redshift – radio continuum: galaxies – submillimetre

1 INTRODUCTION

There is strong evidence that powerful high redshift radio galaxies (HzRGs; $z > 2$) are the progenitors of the brightest cluster ellipticals seen today. HzRGs are the infrared brightest and presumably the most massive galaxies at any epoch (De Breuck et al. 2002) and host actively-accreting super massive black holes with masses of order $10^9 M_\odot$ (Lacy et al. 2001; Dunlop et al. 2003). Therefore, they are key objects for studying the formation and evolution of massive galaxies and super-massive black holes.

HzRGs are likely to be in an important phase of their formation process for several reasons: They have large reservoirs of gas from which they could be forming, as shown by spectacular (> 100 kpc) luminous $\text{Ly}\alpha$ haloes (e.g., McCarthy 1993; van Ojik et al. 1996; Reuland et al. 2003) and widespread H I absorption features in the $\text{Ly}\alpha$ profiles (van Ojik et al. 1997). Their rest-frame UV mor-

phologies are characterized by clumpy structures, similar to the Lyman-break galaxies at $z \sim 3$, that will merge with the central galaxy on dynamical time-scales of 10^8 yrs (Pentericci et al. 1998, 1999). In the case of 4C 41.17 there is direct evidence for massive star formation (up to $\sim 1500 M_\odot \text{yr}^{-1}$ after correction for extinction) based on stellar absorption-lines (Dey et al. 1997). Finally, mm-interferometry studies of CO line and continuum emission for three $z > 3$ HzRGs have shown that the star formation occurs galaxy wide over distances up to 30 kpc (Papadopoulos et al. 2000; De Breuck et al. 2003) and there is even evidence for star formation on scales of 250 kpc (Stevens et al. 2003). Together this suggests that we are observing not merely scaled up versions of local ultraluminous infrared galaxies (ULIRGs) where the bursts are confined to the inner few kpc, but wide-spread starbursts within which the galaxies are forming the bulk of their eventual stellar populations.

HzRGs are an important sample for studying the star formation history of the universe because their selection is

* E-mail: reuland@strw.leidenuniv.nl

based on long wavelength radio emission whose propagation is not affected by the presence of dust. Dust is expected to play a significant role in star forming regions, absorbing UV/optical radiation from the starburst and reradiating it at far-infrared (FIR) wavelengths (Sanders & Mirabel 1996). Optical searches for distant galaxies (e.g., using the Lyman-break technique; Steidel et al. 1996, 1999; Ouchi et al. 2001) are thus likely to be biased against dusty objects. Finding distant star forming galaxies through submillimetre (submm; rest-frame FIR) emission (e.g., Hughes et al. 1998; Bertoldi et al. 2002; Chapman et al. 2002a; Cowie et al. 2002; Scott et al. 2002; Smail et al. 2002; Webb et al. 2003a; Eales et al. 2003) selects only the most obscured sources. So far there has been little overlap between the optical and submm selected star forming sources (selection on very red near-IR colours may prove more fruitful; e.g., Frayer et al. 2004). It remains unclear whether they are members of a continuous population (e.g., Adelberger & Steidel 2000; Webb et al. 2003b) and arguments have been made that either could dominate the star formation density at high redshift (Blain et al. 1999; Adelberger & Steidel 2000). Since selection at radio wavelengths circumvents the aforementioned selection biases it could help determine the relative contributions of obscured and unobscured star formation to the star formation history of the universe.

Archibald et al. (2001, hereafter A01) have conducted the first systematic submm survey to study the star formation history of radio galaxies over a redshift interval of $0.7 < z < 4.4$. In their sample of 47 galaxies, they found evidence for a considerable range in FIR luminosities, a substantial increase in $850\ \mu\text{m}$ detection rate with redshift and that the average $850\ \mu\text{m}$ luminosity rises at a rate $(1+z)^{3-4}$ out to $z \simeq 4$. These results prompt the following questions: Is the dispersion in FIR luminosities due to differences in their star formation rates or dust contents? Does the strong increase with redshift reflect an increase in star formation rates or could it be related to changing dust properties? Does the FIR luminosity keep on rising with redshift or does it level off and is there a redshift cut-off? Are the inferred star formation rates comparable to those derived from the optical/UV? Do the submm properties of quasars (QSOs) and radio galaxies show similar trends or do the two classes of objects evolve differently?

The submm findings from A01 were based on a limited number of detections at high redshift ($z > 3$). To put these results on a statistically firmer footing and search for possible correlations with other galaxy parameters more submm observations were required. Here we present such observations of all $z > 3$ HzRGs known at the beginning of 2001 (e.g., De Breuck et al. 2001) which had not been observed in the submm. Adding these to the survey of A01 almost triples the number of detections at high redshift, creating a sample which is statistically significant over the full redshift range $z = 1 - 5$.

The structure of this paper is as follows: the sample selection, observations and data analysis are described in Section 2. Results and notes on some individual sources are presented in Section 3. Various correlations with submm properties of HzRGs are investigated in Section 4 and described in detail in Section 5. Section 6 presents a comparison between HzRGs and QSOs. We discuss and sum-

marize our conclusions in Section 7. Throughout this paper, we adopt a flat universe with $\Omega_M = 0.3$, $\Omega_\Lambda = 0.7$, and $H_0 = 65\ \text{km s}^{-1}\ \text{Mpc}^{-1}$. Using this cosmology the look-back time at $z \sim 2.5$ (the median redshift of our sample) is $11.7\ h_{65}^{-1}\ \text{Gyr}$ and a galaxy at such a redshift must be less than $2.8\ h_{65}^{-1}\ \text{Gyr}$ old.

2 SAMPLE SELECTION AND OBSERVATIONS

The observations presented here include submm observations of distant radio galaxies. The targets were selected from an increasing sample of HzRGs that is the result of an ongoing effort by our group and others (De Breuck et al. 2000a, 2001, de Vries et al. in preparation; Spinrad private communication) to find distant radio galaxies based on Ultra Steep Radio Spectrum (USS; i.e. red radio color) and near-IR identification selection criteria (for details see De Breuck et al. 2001).

We selected all HzRGs known at the beginning of 2001 with redshifts $z \gtrsim 3$ and declination $\delta > -30^\circ$ that did not have prior submm observations. Our aim was to observe a significant sample of HzRGs to complement the observations of A01 and, in particular, to obtain better statistics at the highest redshifts. MG 2141+192 and 4C 60.07 were observed in both programs, because, at the time of observation, their inclusion in the A01 sample was unknown to us. The $850\ \mu\text{m}$ results for B3 J2330+3927, 6C J1908+722, and 4C 60.07 have been published previously as part of their CO imaging studies (Papadopoulos et al. 2000; De Breuck et al. 2003). MRC 1138–262 was included in the program because of its wealth of supporting data (e.g., Pentericci et al. 1997; Carilli et al. 2002) and WN J1115+5016 because it is one of only two radio galaxies showing a broad absorption line (BAL) system (De Breuck et al. 2001), the other BAL radio galaxy, 6C J1908+722, being a strong CO emitter (Papadopoulos et al. 2000). WN J0528+6549 at $z = 1.210$ was observed because it was first thought to be at redshift $z = 3.120$ (actually belonging to another galaxy on the slit).

The coordinates, redshifts, largest angular sizes of the radio sources, $\text{Ly}\alpha$ fluxes, K -band magnitudes, and references for the full sample observed in the submm are listed in Table 1.

2.1 SCUBA photometry

The observations were carried out between October 1997 and January 2002 with the Submillimetre Common–User Bolometer Array (SCUBA; Holland et al. 1999) at the 15 m James Clerk Maxwell Telescope (JCMT). We observed at $450\ \mu\text{m}$ and $850\ \mu\text{m}$ wavelengths resulting in beam sizes of $7.5''$ and $14.7''$ respectively. We employed the 9-point jiggle photometry mode, which samples a 3×3 grid with $2''$ spacing between grid points, while chopping $45''$ in azimuth at 7.8 Hz. Frequent pointing checks were performed to ensure pointings better than $2''$ and reach optimal sensitivity.

Our original goal was to observe all sources down to 1 mJy rms at $850\ \mu\text{m}$. This is a sensible limit, since at $850\ \mu\text{m}$ confusion becomes a problem for sources weaker than 2 mJy (Hughes et al. 1998; Hogg 2001), it is obtainable in 3 hrs per source, and it is matched to the survey by A01. However, because of scheduling constraints, and because our priority

Table 1. Redshifts, radio positions, largest angular sizes, Ly α fluxes, K -band magnitudes and references to papers from which these data were taken for all objects that were observed in our submm program. The Ly α fluxes are in units of 10^{-16} erg s $^{-1}$ cm $^{-2}$, and the K -band magnitudes were measured in a 64 kpc diameter aperture where possible. References: DB99, DB00a, DB00b, DB01, DB02, DB03a, DB03b = De Breuck et al. (1999, 2000a, b, 2001, 2002, 2003, De Breuck et al. in preparation), dV03 = de Vries et al. in preparation, Dey99 = Dey (1999), Dri97 = Drinkwater et al. (1997), ER96 = Eales & Rawlings (1996), McC90 = McCarthy et al. (1990), McC96 = McCarthy et al. (1996), Kap98 = Kapahi et al. (1998), Pap00 = Papadopoulos et al. (2000), Pen97 = Pentericci et al. (1997), Ren98 = Rengelink (1998), Röt97 = Röttgering et al. (1997), S99 = Stern et al. (1999), vB99 = van Breugel et al. (1999).

Source	z	RA(J2000)			DEC (J2000)			LAS "	$F_{\text{Ly}\alpha}$ cgs	K mag	References
		h	m	s	°	'	"				
WNJ0528+6549	1.210	5	28	46.07	+ 65	49	57.3	1.9	–	18.2	DB00a, dV03
MRC1138–262	2.156	11	40	48.25	– 26	29	10.1	15.8	13.9	16.1	Röt97, Pen97, DB00b
WNJ1115+5016	2.550	11	15	6.87	+ 50	16	23.9	0.2	2.0	19.2	DB00a, DB01, DB02
WNJ0747+3654	2.992	7	47	29.38	+ 36	54	38.1	2.1	0.8	20.0	DB00a, DB01, DB02
WNJ0231+3600	3.079	2	31	11.48	+ 36	0	26.6	14.8	1.1	–	DB00a, DB01, DB02
B3J2330+3927	3.086	23	30	24.91	+ 39	27	11.2	1.9	4.4	18.8	DB03a
TNJ1112–2948	3.090	11	12	23.86	– 29	48	6.2	9.1	2.9	–	DB00a, DB01
MRC0316–257	3.130	3	18	12.06	– 25	35	9.7	7.6	2.4	–	McC90, ER96, DB00b
PKS1354–17	3.150	13	47	96.03	– 17	44	02.2	–	–	–	Dri97
WNJ0617+5012	3.153	6	17	39.37	+ 50	12	54.7	3.4	0.8	19.7	DB00b, DB01, DB02
MRC0251–273	3.160	2	53	16.70	– 27	9	9.6	3.9	–	–	McC96, Kap98
WNJ1123+3141	3.217	11	23	55.85	+ 31	41	26.1	25.8	6.2	17.5	DB00a, DB01, DB02
WNH1702+6042	3.223	17	3	36.23	+ 60	38	52.2	11.5	–	–	Ren98
TNJ0205+2242	3.506	2	5	10.69	+ 22	42	50.3	2.7	–	18.8	DB00a, DB01, DB02
TNJ0121+1320	3.516	1	21	42.74	+ 13	20	58.3	0.3	–	18.8	DB00a, DB01, DB02
6C1908+722	3.532	19	8	23.70	+ 72	20	11.8	14.4	32.0	16.5	Dey99, Pap00, DB01
WNJ1911+6342	3.590	19	11	49.54	+ 63	42	9.6	1.8	1.4	18.6	DB00a, DB01, DB02
MG2141+192	3.592	21	44	7.50	+ 19	29	15.0	8.5	6.2	19.3	S99
WNJ0346+3039	3.720	3	46	42.68	+ 30	39	49.3	0.4	–	17.8	DB00a, DB02, dV03
4C60.07	3.791	5	12	55.15	+ 60	30	51.0	16.0	10.1	19.3	Röt97, Pap00, DB00b
TNJ2007–1316	3.830	20	7	53.23	– 13	16	43.6	7.2	2.5	17.9	DB00a, DB02, DB03b
TNJ1338–1942	4.100	13	38	26.06	– 19	42	30.1	5.5	10.1	19.7	DB99
TNJ1123–2154	4.109	11	23	10.15	– 21	54	5.3	0.8	0.2	20.4	DB00a, DB01, DB02
TNJ0924–2201	5.190	9	24	19.92	– 22	1	41.5	1.2	0.4	19.9	vB99

was to obtain a large sample of HzRGs with 850 μm detections, this limit was not always reached. Rather, the next target was observed as soon as an apparent 5σ detection had been obtained at 850 μm .

The atmospheric optical depths τ_{850} , τ_{450} were calculated using the empirical CSO–tau correlations given by Archibald et al. (2002), unless the values obtained through skydips disagreed strongly, in which case those were used instead. The optical depth τ_{850} varied between 0.14 and 0.38 with an average value of 0.26. The data were clipped at the 4σ level to ensure accurate determination of the sky level, flat-fielded, corrected for extinction, sky noise was removed after which they were co-added and clipped at the 2.5σ level using the Scuba User Reduction Facility software package (SURF; Jenness & Lightfoot 1998), following standard procedures outlined in the SCUBA Photometry Cookbook¹. The concatenated data were checked for internal consistency using a Kolmogorov–Smirnov (K–S) test and severely deviating measurements (if any) were removed. Finally, flux calibration was performed using HLTAU, OH231.8 and CRL618 as photometric calibrators. The typical photometric uncertainty for our program is of order 10–15 per cent, as estimated from our results on three sources (TN J0121+1320,

TN J1338–1942, and MG 2141+192) that were observed at two separate instances each. This photometric accuracy is consistent with an estimated 10 per cent systematic uncertainty in the 850 μm flux density scale (see e.g., Papadopoulos et al. 2000; Jenness et al. 2001). Given that HzRGs appear to be located in submm overdense regions (e.g., Stevens et al. 2003) flux may have been lost due to chopping onto a nearby galaxy. However this very unlikely to have affected more than a few sources.

Following Omont et al. (2001), Table 2 includes a column indicating the quality of the observation. Good quality data is indicated by an ‘A’, whereas poor quality is indicated by a ‘B’. Poor quality reflects bad atmospheric conditions (e.g. large seeing), short integration time (< 2 sets of 50 integrations each), or poor internal consistency as shown by the K–S test (i.e. the measurements were not consistent, but it was impossible to determine which were the outliers. In such cases the average of all measurements was used).

2.2 Potential contamination of the thermal submillimetre flux

Because all our objects are powerful radio galaxies, it is important to estimate any synchrotron contribution to the observed submm band. We used flux densities from the WENSS (325 MHz Rengelink et al. 1997), Texas (365 MHz; Douglas et al. 1996) and NVSS (1.4 GHz; Condon et al.

¹ The SCUBA Photometry Cookbook is available at <http://www.starlink.rl.ac.uk/star/docs/sc10.htx/sc10.html>

1998) surveys to extrapolate to 350 GHz (850 μm) frequencies using a power law. For 53W069, we extrapolated from the 600 MHz and 1.4 GHz values in Waddington et al. (2000). We find that the synchrotron contribution at 850 μm is negligible for most galaxies in our sample. Only for some objects from A01 (and PKS 1354–17) would this require corrections larger than the 1σ uncertainties in the 850 μm measurements.

Synchrotron spectra often steepen at high frequencies (e.g., A01; Athreya et al. 1997; Andreani et al. 2002; Sohn et al. 2003), and linear extrapolation should be considered an upper limit to the synchrotron contribution. A01 performed parabolic fits to account for the curvature of the radio spectrum. Using the midpoint between linear and parabolic fits they find corrections larger than 1.5 mJy to the 850 μm flux densities in only 6 cases. One could argue that parabolic fits are more appropriate, in which case all corrections would be negligible.

Note that the radio measurements reflect the spatially integrated flux densities of the sources. The radio cores have flatter spectra than the lobes and could dominate at higher frequencies. However, they are usually faint and for USS sources even the radio cores tend to have steep spectra (e.g., A01; Athreya et al. 1997) indicating that contamination by the core is likely to be negligible as well.

Given these uncertainties, extrapolation from the radio regime to submm wavelengths is uncertain and is likely to result in an overestimate of the non-thermal contribution due to steepening of the radio spectrum. This is demonstrated for the case of B3 J2330+3927, for which De Breuck et al. (2003) estimate a non-thermal contribution of ~ 1.3 mJy at 113 GHz but measured a flux density < 0.3 mJy that seems to be of thermal origin. Therefore we do not correct for a contribution to the submm continuum from the non-thermal radio emission, except for a few sources discussed below. For these reasons (and following Willott et al. 2002) we have chosen also to use uncorrected fluxes from A01 in the remainder of this paper.

There are two exceptions that we exclude from our final sample. Following A01, we reject B2 0902+34, as this source has a bright flat-spectrum radio core which could dominate the submm emission. We also reject the flat spectrum radio source PKS 1354–17. It is significantly brighter than any of the other sources at 850 μm ($S_{850} = 20.5 \pm 2.6$ mJy), but linear extrapolation from the radio regime shows that the non-thermal contribution at 850 μm could be as large as 40 mJy and could easily account for all of the submm signal.

Gravitational lensing may be important in some cases (Lacy 1999), resulting in enhanced submm fluxes. However, recent estimates (e.g., Chapman et al. 2002b; Dunlop et al. 2002) show that this is limited to a small but significant fraction (3–5 per cent of sources with $S_{850} > 10$ mJy may have been boosted by a factor $\gtrsim 2$) and that for most objects there is no evidence for strong gravitational lensing. Corrections for lensing must be made on a case-to-case basis and are strongly model dependent. Since these corrections are likely to be small, they have not been attempted for the present sample.

2.3 Dust template

As has been noted by many authors (e.g., A01; Hughes et al. 1997), choosing the dust template is an important step in inferring the bolometric far infra-red luminosities (L_{FIR}), star formation rates (SFR) and dust masses (M_{d}). A complication is that the appropriate dust template may change over redshift due to changing dust properties with the evolutionary states of the galaxies.

Throughout this paper we adopt single temperature, optically thin greybody emission for two sets of emissivity index β and temperature T_{d} (see Dunne & Eales 2001; Dupac et al. 2003, for possible concerns) as the functional parametrization for thermal dust emission from high redshift sources. We choose $\beta = 1.5$ and $T_{\text{d}} = 40$ K for comparison with other papers (e.g., A01; and see Dunne et al. 2000; Eales et al. 2003), and also briefly investigate the effects of assuming $\beta = 2.0$ and $T_{\text{d}} = 40$ K as seems reasonable for some hyperluminous IR galaxies ($T_{\text{d}} = 35$ K; HyLIRGs Farrah et al. 2002) and $z > 4$ quasars ($T_{\text{d}} = 40$ –50 K; Priddey & McMahon 2001; Willott et al. 2002). Measuring the value of β for HzRGs directly would require observations at many more rest-frame FIR wavelengths than presented here. Increasing β or the dust temperature decreases the inferred L_{FIR} of high redshift sources relative to lower redshift sources for a given flux density.

The fraction of absorbed UV/optical light, δ_{SB} , and possible departures from the prototype Salpeter initial mass function, parametrized with δ_{IMF} , are other uncertain factors. Generally accepted approximations (see e.g., Papadopoulos et al. 2000; Omont et al. 2001; De Breuck et al. 2003) for the dust mass, inferred FIR luminosity and star formation rate are respectively:

$$M_{\text{d}} = \frac{S_{\text{obs}} D_{\text{L}}^2}{(1+z)\kappa_{\text{d}}(\nu_{\text{rest}})B(\nu_{\text{rest}}, T_{\text{d}})},$$

$$L_{\text{FIR}} = 4\pi M_{\text{d}} \int_0^{\infty} \kappa_{\text{d}}(\nu) B(\nu, T_{\text{d}}) d\nu =$$

$$\frac{8\pi h}{c^2} \frac{\kappa_{\text{d}}(\nu)}{\nu^{\beta}} \left(\frac{kT}{h}\right)^{\beta+4} \Gamma(\beta+4)\zeta(\beta+4)M_{\text{d}},$$

and

$$\text{SFR} = \delta_{\text{IMF}} \delta_{\text{SB}} (L_{\text{FIR}}/10^{10} L_{\odot}) M_{\odot} \text{ yr}^{-1},$$

with $\kappa_{\text{d}}(\nu) \propto \nu^{\beta}$ the frequency dependent mass absorption coefficient which modifies the Planck function, $B(\nu, T_{\text{d}})$, to describe the isothermal greybody emission from dust grains, Γ the Gamma function, ζ the Riemann Zeta function, D_{L} the luminosity distance and S_{obs} the observed flux density. The mass absorption coefficient is poorly constrained (e.g., Chini et al. 1986; Downes et al. 1992; De Breuck et al. 2003; James et al. 2002) and we conform to the intermediate value of $\kappa_{\text{d}}(375\text{GHz}) = 0.15 \text{ m}^2 \text{ kg}^{-1}$ chosen by A01.

3 OBSERVATIONAL RESULTS

24 radio sources were observed. The results of the observations, the inferred rest-frame 850 μm luminosities L_{850} , total far-IR luminosities L_{FIR} , and radio luminosities $L_{3\text{GHz}}$ are summarized in Table 2. 12 of the HzRGs are detected at $>3\sigma$

significance at 850 μm . The median rms flux density of the observations is $\sigma_{850} = 1.5 \text{ mJy}$ with an interquartile range of 0.8 mJy. Only B3 J2330+3927 may have been detected at 450 μm at a 2σ level ($S_{450} = 49.1 \pm 17.7 \text{ mJy}$).

Particularly noteworthy is MG 2141+192. This source was detected by A01 at the 4.8σ -level at $S_{850} = 4.61 \pm 0.96 \text{ mJy}$, using the narrow filterset whereas we observed $S_{850} = 2.16 \pm 1.10 \text{ mJy}$ and $S_{850} = 2.45 \pm 1.58 \text{ mJy}$ at two separate instances with the wide filter set and did not detect the source. Similarly 4C 60.07 has been detected in photometry mode at $S_{850} = 11.5 \pm 1.5$, 17.1 ± 1.3 and in a jiggle map at 21.6 ± 1.3 (A01; Papadopoulos et al. 2000; Stevens et al. 2003). These measurements are consistent to within $2\text{--}3\sigma$ from the mean. However, naively, they could also be interpreted as signs of submm variability. A01 and Willott et al. (2002) also found tentative evidence for variability in the submm, but ascribed it to problems with sky subtraction for data obtained with the single-element bolometer UKT14 versus SCUBA. It is hard to see how widespread star formation could result in submm variability on the time-scale of years. Significant changes in L_{FIR} might be easier to envisage as the result of UV variability often seen in AGN and if the submm emission results from quasar heated dust. However, even in this scenario changes in the UV are expected to average over time in the observed submm regime, unless the FIR emitting region is compact. While the typical scale sizes for UV emission from the AGN are on parsec scales, the minimum extent of the FIR emitting region must be about 1 kpc to match the observed luminosity and dust temperature (e.g., Carilli et al. 2001). Submm variability, if real, is therefore hard to explain if reprocessing by dust is the dominant mechanism for the FIR emission. If, alternatively, the FIR emission would be non-thermal emission from the AGN, then the emission should be unresolved in contrast to the observed extents of a few tens of kpc. Moreover, observations indicate that AGN contribute at most 30 per cent of the FIR luminosity at wavelengths longer than 50 μm , at least for HyLIRGs (Rowan-Robinson 2000; Farrah et al. 2002).

Possible explanations therefore may be that (i) for different chopping angles and distances sometimes flux is accidentally lost due to companion galaxies in the off-beam since the fields are overdense (Stevens et al. 2003), or (ii) that sometimes the AGN do in fact contribute close to the maximum amount expected (note that the submm flux for 4C 60.07 is centrally concentrated; Fig. 2 in Stevens et al. 2003), even though the starbursts still dominate. (iii) Finally of course there is still the possibility of pointing errors, uncertainties in absolute flux calibration, and differences in atmospheric transparency that could shift the effective bandpass by a few GHz, which could make a difference due to the very steep slope of the spectrum.

4 ANALYSIS

In the following we discuss a sample of 67 radio galaxies (46/47 from A01, 23/24 from this paper, two sources were observed in both samples). This excludes the flat-spectrum sources B2 0902+34 and PKS 1354–17 (see Section 2.2). For the statistical analysis we use the inverse variance weighted averages of the measurements of MG 2141+192 ($\langle S_{850} \rangle =$

$3.3 \pm 0.7 \text{ mJy}$) and 4C 60.07 ($\langle S_{850} \rangle = 14.4 \pm 1.0 \text{ mJy}$) and for MRC 1138–262 we prefer the value of $S_{850} = 5.9 \pm 1.1 \text{ mJy}$ obtained by Stevens et al. (2003) over our observation under adverse conditions. The median rms flux density for this entire sample is $\sigma_{850} = 1.1 \text{ mJy}$ with a 0.24 mJy interquartile range.

Figure 1 shows that the observed submm flux densities and therefore the inferred luminosities (see Table 2) at $z > 3$ vary significantly from object to object. For the assumed dust template we find a range from $L_{\text{FIR}} < 4 \times 10^{12} L_{\odot}$ for undetected targets to $L_{\text{FIR}} \sim 2 \times 10^{13} L_{\odot}$ for detected sources. There are several viable scenarios to explain this. First, if all the warm dust is heated solely by young stars, then L_{FIR} is linked to the SFR, implying that the SFR differs significantly between objects. Alternatively, there may be a range in produced dust masses as substantial dust production may take more than a billion years if low-mass stars are the principal contributors (e.g., Edmunds 2001). In this case the range in L_{FIR} may reflect a range in starburst ages. The recent detection of significant amounts of dust in the local supernova remnant Cassiopeia A (Dunne et al. 2003), indicates that much faster evolving massive stars may be at least as important in producing dust. A considerable contribution from high-redshift supernovae would significantly lower the required time-scales for dust production and would favor a range in SFRs to explain the range in L_{FIR} .

Despite the various uncertainties, the result that the far infrared luminosities are high is robust. This has important implications for the starburst nature of these galaxies: inserting the values for L_{FIR} that we find using either dust template confirms that HzRGs are vigorously forming stars up to rates of a few $1000 M_{\odot} \text{ yr}^{-1}$ and have dust masses of a few times $10^8 M_{\odot}$. This is consistent with the notion that they are in a critical phase of their formation, forming the bulk of their stellar masses.

4.1 Statistical analysis

We have performed statistical tests to search for possible correlations of the submm with other properties of the radio galaxies. Specifically, we investigated whether there are correlations with redshift (as reported by A01), radio luminosity (as indicator of AGN contribution), largest angular size of the radio source (as indicator of age), K -band magnitude (as indicator of stellar mass or star formation rate), $\text{Ly}\alpha$ flux (as a possible indicator of starburst “fuel”), and UV polarisation (as indicator of the relative contributions of starburst and AGN to the UV continuum). Below, we discuss these in more detail.

Since the sample contains a large fraction (of order 50 per cent) of non-detections (i.e. upper limits) we have conducted survival analysis tests similar to A01. Survival analysis allows the mixing of detections and upper limits (“censored data points”) in a statistically meaningful way thereby preserving as much information as possible. The results of the survival tests are summarized in Tables 3 and 4. Table 3 represents the results for the entire sample, whereas Table 4 only considers the 32 galaxies with redshifts $z > 2.5$.

We have defined the subsample with redshift $z > 2.5$ to test for selection effects and remove them from our sample. The well known and strong (see A01) radio power-redshift relation in flux limited samples is likely to be the origin of

Table 2. Observed 850 μm and 450 μm submm flux densities $S_{850\ \mu\text{m}}$ and $S_{450\ \mu\text{m}}$ with their standard errors for the radio sources in the program. The total duration of the observations, N_{int} is given in sets of 50 integrations. 3σ upper limits to the 850 μm flux are shown for sources whose S/N is below 3. Only B3 J2330+3927 may have been detected at 2σ at 450 μm . Logarithms of inferred rest-frame 850 μm luminosities L_{850} , far-IR luminosities, L_{FIR} and radio luminosities $L_{3\text{GHz}}$ are shown for the dust template with $\beta = 1.5$, $T_{\text{d}} = 40\text{ K}$ and a flat universe with $\Omega_{\text{M}} = 0.3$, $\Omega_{\Lambda} = 0.7$, and $H_0 = 65\text{ km s}^{-1}\text{ Mpc}^{-1}$.

Source	z	$N_{\text{int}} \times 50$	S_{850}^a mJy	S/N	Quality	3σ lim. mJy	S_{450} mJy	L_{850} $\text{W Hz}^{-1}\text{ sr}^{-1}$	L_{FIR} L_{\odot}	$L_{3\text{GHz}}$ $\text{W Hz}^{-1}\text{ sr}^{-1}$
WNJ0528+6549	1.210	4+4	-1.9 ± 1.3	-1.4	A	<3.9	2 ± 29	<23.05	<12.63	24.59
MRC1138-262	2.156	2	12.8 ± 3.3^b	3.9	B		-65 ± 134	23.26 ^b	12.83 ^b	27.15
WNJ1115+5016	2.550	4	3.0 ± 1.3	2.3	A	<6.9	-20 ± 11	<23.31	<12.90	25.95
WNJ0747+3654	2.990	6	4.8 ± 1.1	4.5	A		18 ± 15	23.15	12.73	26.22
WNJ0231+3600	3.080	7	5.9 ± 1.6	3.7	B		-29 ± 22	23.23	12.81	26.27
B3J2330+3927	3.086	3	14.1 ± 1.7^c	8.5	A		49 ± 18	23.61	13.19	26.56
TNJ1112-2948	3.090	5	5.8 ± 1.1	5.1	A		15 ± 9	23.23	12.81	26.66
MRC0316-257	3.130	2	0.6 ± 2.7	0.2	B	<8.8	5 ± 48	<23.41	<12.99	27.22
PKS1354-17	3.150	2	20.5 ± 2.6^d	8.0	B		-47 ± 77	23.77	–	27.71
WNJ0617+5012	3.153	6+6	1.0 ± 0.7	1.3	B	<3.2	3 ± 16	<22.96	<12.55	26.10
MRC0251-273	3.160	2	0.6 ± 2.8	0.2	A	<8.9	-54 ± 91	<23.41	<12.99	27.00
WNJ1123+3141	3.220	8	4.9 ± 1.2	4.1	A		4 ± 14	23.15	12.73	26.60
WNH1702+6042	3.223	1	-0.4 ± 3.6	-0.1	B	<10.8	-73 ± 91	<23.49	<13.07	26.40
TNJ0205+2242	3.506	6	1.3 ± 1.3	1.0	A	<5.2	27 ± 23	<23.17	<12.75	26.58
TNJ0121+1320	3.517	7+4	7.5 ± 1.0	7.6	A		4 ± 16	23.33	12.91	26.55
6CJ1908+722	3.532	6	10.8 ± 1.2^e	9.0	A		33 ± 17	23.49	13.07	27.25
WNJ1911+6342	3.590	2	1.3 ± 3.6	0.4	B	<11.9	-38 ± 50	<23.53	<13.11	26.26
MG2141+192	3.592	7+5	$2.3 \pm 0.9^{b,e}$	2.6	A	<5.0	12 ± 13	22.96 ^b	<12.55 ^b	27.30
WNJ0346+3039	3.720	4	-0.5 ± 1.3	-0.4	A	<3.8	-5 ± 12	<23.02	<12.61	26.43
4C60.07	3.791	5	$11.5 \pm 1.5^{b,c,e}$	7.6	A		10 ± 13	23.61 ^b	13.19 ^b	27.15
TNJ2007-1316	3.830	5	5.8 ± 1.5	4.0	A		4 ± 45	23.21	12.79	26.98
TNJ1338-1942	4.100	4+7	6.9 ± 1.1	6.2	A		-36 ± 32	23.29	12.87	27.05
TNJ1123-2154	4.109	2	1.5 ± 1.7	0.9	A	<6.7	-7 ± 11	<23.27	<12.85	26.76
TNJ0924-2201	5.190	8+4	-0.7 ± 1.1	-0.7	A	<3.2	-0 ± 26	<22.94	<12.53	27.24

^aThis does not include the 10–15 per cent uncertainty in absolute photometric calibration.

^bFor the statistical analysis we use $S_{850} = 5.9 \pm 1.1\text{ mJy}$, $S_{850} = 3.3 \pm 0.7\text{ mJy}$ and $S_{850} = 14.4 \pm 1.0\text{ mJy}$ for MRC 1138–262, MG 2141+192 and 4C 60.07, respectively. L_{850} and L_{FIR} were inferred using those values. See Section 4 for details.

^cData published in CO imaging studies by Papadopoulos et al. (2000) and De Breuck et al. (2003).

^dPKS 1354–17 is likely to be dominated by non-thermal emission (c.f. Section 2.2).

^eAlso part of the survey by A01.

Table 3. Results of survival analysis for all 67 sources. The significance P is the probability of the variables not being correlated according to each test. If all three tests yield $P \lesssim 5$ per cent, then the variables are taken to be correlated. If only some yield $P \lesssim 5$ per cent then a correlation is regarded as possible, but uncertain. Results are shown for both a 3σ and 2σ (between brackets) detection limit.

Variable	Dependent	Independent	Percentage of Data Censored	Cox	Significance (P) Kendall	Spearman	Correlation Present?
$S_{850\ \mu\text{m}}$		z	67% (52)%	0% (0%)	0% (0%)	0% (0%)	YES (YES)
D_{lin}		$L_{3\ \text{GHz}}$	0%	17%	34%	32%	NO
$L_{3\ \text{GHz}}$		z	0%	1%	2%	2%	YES
$L_{850\ \mu\text{m}}$		$L_{3\ \text{GHz}}$	67% (52)%	1% (1%)	7% (8%)	10% (8%)	MAYBE (MAYBE)
$L_{850\ \mu\text{m}}$		z	67% (52)%	0% (0%)	0% (0%)	0% (0%)	YES (YES)
$L_{850\ \mu\text{m}}$		α	67% (52)%	1% (1%)	1% (0%)	1% (0%)	YES (YES)
$L_{850\ \mu\text{m}}$		D_{lin}	67% (52)%	56% (22%)	79% (89%)	96% (78%)	NO (NO)
α		$L_{3\ \text{GHz}}$	0%	36%	20%	19%	NO
α		z	0%	0%	0%	0%	YES

many apparent correlations with redshift (see Table 3). Another example of selection effects is the correlation found between L_{850} and radio spectral index α (Table 3). It reflects the tight correlations between spectral index and redshift (part of our search criteria for HzRGs) and between L_{850} and redshift. In the $z > 2.5$ sample this correlation almost disappears even though there is a large range in both L_{850} and α , confirming that it was spurious. An additional advan-

tage of this subsample is the homogeneity of the supporting data (Ly α fluxes and K -band magnitudes are understandably sparse for lower redshift sources).

Below, we describe the details of the survival analysis and the criteria used to determine whether a correlation is present. In Section 5, we discuss the correlations individually.

Table 4. Similar to Table 3. Results of survival analysis for 32 sources at redshifts $z > 2.5$.

Variable		Percentage of Data Censored	Cox ^a	Significance (P)		Correlation Present?
Dependent	Independent			Kendall	Spearman	
$S_{850\mu\text{m}}$	z	53% (34%)	95% (81%)	17% (25%)	34% (38%)	NO (NO)
D_{lin}	$L_{3\text{GHz}}$	0%	66%	8%	9%	NO
$L_{3\text{GHz}}$	z	0%	7%	4%	4%	MAYBE
$L_{850\mu\text{m}}$	$L_{3\text{GHz}}$	53% (34%)	21% (33%)	33% (48%)	46% (58%)	NO (NO)
$L_{850\mu\text{m}}$	z	53% (34%)	88% (75%)	20% (34%)	35% (52%)	NO (NO)
$L_{850\mu\text{m}}$	α	53% (34%)	88% (99%)	81% (69%)	99% (71%)	NO (NO)
$L_{850\mu\text{m}}$	D_{lin}	53% (34%)	13% (6%)	16% (7%)	13% (6%)	NO (NO)
$L_{850\mu\text{m}}$	$L_{\text{Ly}\alpha}$	59% (41%)	–	86% (91%)	4% (4%)	MAYBE (MAYBE)
$L_{850\mu\text{m}}$	Kmag	59% (44%)	–	47% (33%)	88% (72%)	NO (NO)
α	$L_{3\text{GHz}}$	0%	56%	21%	11%	NO
α	z	0%	2%	10%	8%	MAYBE

^a Cox's proportional hazard model only allows censoring in the dependent variable, therefore this test could not be applied with the Ly α and K-band data.

Survival analysis

The application of survival analysis methods to astronomical data has been described in detail by Feigelson & Nelson (1985) and Isobe et al. (1986). We have made use of the routines in the STSDAS package of IRAF² (Tody 1993), which were modelled after the ASURV package (Lavalley et al. 1992). Cox's proportional hazard model, the generalized Spearman's rank order correlation coefficient, and the generalized Kendall's tau correlation coefficient test the null hypothesis that no correlation is present in the sample. We adopt the convention that two variables are correlated if the chance P of the null hypothesis being true is smaller than 5 per cent. While these tests should give similar results they have different specific limitations and strong points. Therefore, a correlation is considered to be reliable if all tests yield $P \lesssim 5$ per cent, and possible but unconfirmed if only some indicate $P \lesssim 5$ per cent. Note that the Cox test only allows censoring in the dependent variable and that the generalized Spearman's Rho routine is not reliable for small data sets ($N < 30$). SCUBA occasionally yields negative flux densities. We defined the $n\sigma$ upperlimit for those cases to be $n \times$ the rms flux density. Similarly, the $n\sigma$ upperlimit for a positive signal is defined as $S + n \times$ the rms flux density, with S the observed signal.

5 CORRELATIONS BETWEEN PARAMETERS

Tables 3 and 4 represent the results of the survival analysis as described above. We will now discuss the motivation for each test and the implications of the correlations (or lack thereof) found in order of importance.

² IRAF is distributed by the National Optical Astronomy Observatories, which are operated by the Association of Universities for Research in Astronomy, Inc., under cooperative agreement with the National Science Foundation.

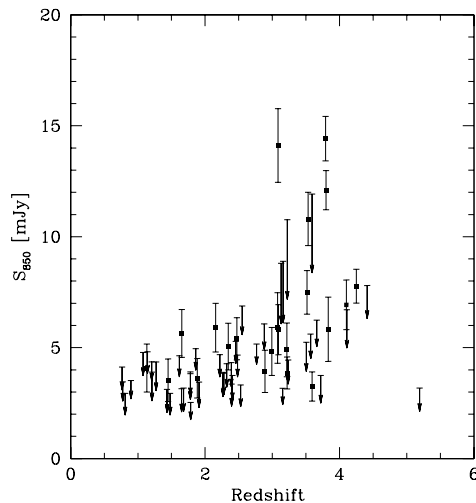


Figure 1. Observed 850 μm flux density and 3σ upper limits versus redshift of all 67 radio galaxies discussed in this paper. The size of the arrows and errorbars correspond to 1σ rms.

5.1 Redshift dependent submillimetre properties

5.1.1 Flux density and relative detection fraction

Table 3 shows that the observed submm flux densities S_{850} are strongly correlated with redshift. This is reflected in Figure 1 and 2. Figure 1 shows the observed 850 μm flux densities against redshift. Figure 2 shows the number of radio galaxies that have been observed in a particular redshift bin and the number of those which have been detected given a 2σ or 3σ detection criterion. The success rate of our $z > 3$ program is truly remarkable, and corroborates the conclusion of A01 that the detection fraction of ~ 50 – 67 per cent at $z > 2.5$ is significantly different from the detection fraction of ~ 15 per cent at $z < 2.5$. Removing the 4 brightest sources from the sample does not destroy this relation.

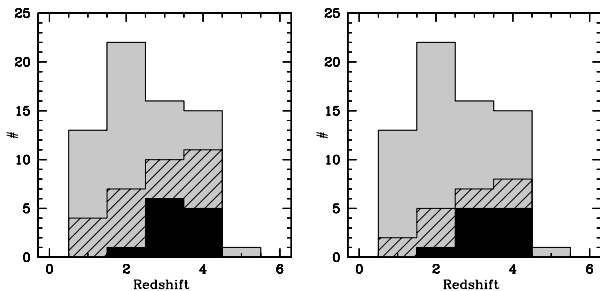


Figure 2. Histograms of 850 μm SCUBA detections with $S/N > 2$ (left) and $S/N > 3$ (right) versus the total number of observed radio galaxies (grey) as a function of redshift. The detections from Archibald et al. (2001) are shown as dashed, the detections from our program are shown in black. At $z > 2.5$ ~ 50 –67 per cent of the galaxies are detected, as opposed to ~ 15 per cent at $z < 2.5$. The bins have a width of unit redshift and are centered at $z = 1, 2, 3, 4, 5$.

5.1.2 Investigation of the difference between detections and non-detections

Given a 3σ detection criterion the average submm flux density of the 22 detected radio sources and 45 non-detections are $\langle S_{850, \geq 3\sigma} \rangle = 6.60 \pm 0.71$ mJy and $\langle S_{850, < 3\sigma} \rangle = 0.81 \pm 0.20$ mJy respectively, while the average for the entire sample is $\langle S_{850, \text{sample}} \rangle = 2.71 \pm 0.43$ mJy. For a 2σ detection criterion the average submm flux density of the 30 detected galaxies and 37 non-detections are $\langle S_{850, \geq 2\sigma} \rangle = 5.29 \pm 0.60$ mJy and $\langle S_{850, < 2\sigma} \rangle = 0.34 \pm 0.19$ mJy respectively.

Figure 3 shows cumulative redshift distributions $\Sigma(z)$ for various subsets of the radio galaxy sample together with spectroscopic redshifts for other submm samples from the literature. As was suspected from Figure 2, the radio galaxies detected in the submm follow a distribution that differs significantly from both the undetected sources and the parent sample. The K-S test shows with $P > 99$ per cent confidence that using a 2σ or 3σ detection criterion picks out the same population (both for the detections and for the non-detections), whereas the chance that the detections and non-detections are distributed similarly is $P < 1$ per cent.

Does the high median redshift ($z = 3.1$) of the detected sources (the parent sample has $z = 2.5$) purely reflect the strong negative K -correction or does it reflect a change in L_{FIR} ? Figure 3 shows that the median redshift of the detections is higher than the median redshift ($z = 2.4$) for SCUBA sources (Chapman et al. 2003), while the redshift distribution of the parent sample follows the SCUBA population closely. This argues in favor of a different L_{FIR} for detections and non-detections. What then causes the difference in redshift distribution between detected HzRGs and the submm population? There are at least two possible explanations. It may indicate that HzRGs are more massive, at the centers of protoclusters (Venemans et al. 2003), and therefore undergo a faster evolution than ‘normal’ submm sources and finish the bulk of their formation process early. Alternatively, it may reflect a selection effect as the requirement of a faint radio counterpart prior to spectroscopic follow-up for the submm sample selects against high redshift galaxies (Chapman et al. 2003).

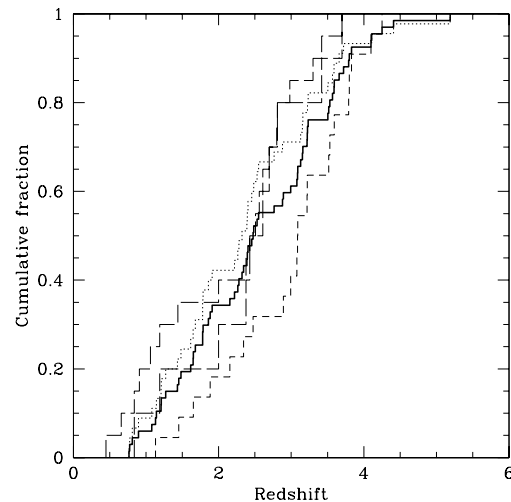


Figure 3. Cumulative histograms $\Sigma N(z)$ for redshifts of submm sources from the literature and the 67 radio galaxies (solid line) discussed in this paper. The short-dashed and the dotted line indicate submm detections of radio galaxies versus non-detections given a 3σ detection criterion, respectively. The detections have a higher median redshift ($z = 3.1$) than the parent sample ($z = 2.5$). The two long-dashed lines represent $\Sigma N(z)$ of the 10 submm sources with spectroscopic redshifts found by Chapman et al. (2003) and using 9 additional spectroscopic redshifts (Ivison et al. 1998, 2000; Dey et al. 1999; Soucail et al. 1999; Eales et al. 2000; Ledlow et al. 2002; Chapman et al. 2002b,c; Aretxaga et al. 2003; Frayer et al. 2003).

5.1.3 The increase of submm luminosity with redshift

Figure 4 shows the inferred 850 μm luminosity L_{850} as a function of redshift. For each redshift bin L_{850} has been estimated using the Kaplan–Maier estimator, a survival analysis technique which tries to estimate the true distribution of the underlying population by incorporating both upperlimits and detections. We have computed the luminosities both using a dust template with $\beta = 1.5$ and $\beta = 2.0$. Adding our data to the sample of A01 confirms that HzRGs have higher submm luminosities than lower redshift sources. However, there are significant differences with the findings from A01: (i) L_{850} at low redshifts is higher than inferred by A01. This is because we have chosen, not to correct for possible synchrotron contamination (see Section 2.3) (ii) There is weak evidence for a turnover or leveling off at $z > 4$ (based on the lower flux densities of the five galaxies with $z > 4$ compared to redshifts $3 < z < 4$; see Fig. 1). This explains why there is no strong correlation between L_{850} and z in the high redshift subsample (see Table 4). (iii) A01 remarked that the increase in L_{850} becomes less pronounced if one assumes a dust template with $\beta = 2$. Because L_{850} at low redshifts is higher than in A01, this effect is even stronger in our sample and we find that L_{850} may be rather constant. The sources would still be highly submm luminous, implying huge dust masses and star formation rates.

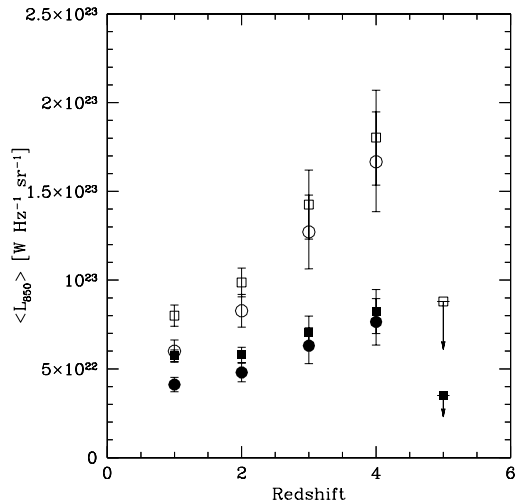


Figure 4. The average rest-frame 850 μm luminosity versus redshift for 67 radio galaxies as estimated using the Kaplan–Maier estimator for each redshift bin. The data points indicated with open squares and circles were calculated assuming the same dust template as A01 ($\beta = 1.5$, $T_d = 40\text{K}$) for 3σ and 2σ detection criteria respectively. The solid symbols are similar but assume $\beta = 2.0$ instead. The data points at $z = 5$ are 3σ upperlimits based on the non-detection of TN J0924–2201.

5.2 The connection between submm and radio luminosity

Radio galaxies host luminous AGNs and for favorable geometries (e.g., dusty warped disks) heating of dust by only a small fraction (≤ 20 per cent) of their UV radiation could easily explain typical far-IR luminosities (e.g., Sanders et al. 1989). Therefore, an important question is: do the AGN heat the large-scale dust significantly, i.e. are L_{radio} and L_{FIR} correlated?

To answer this question we have estimated the rest-frame radio power at 3GHz, $L_{3\text{GHz}}$. We have chosen this frequency because for the redshift range $1.1 < z < 7.2$ this requires only interpolation between between 365 MHz and 1.4 GHz. Of course this assumes that the UV emission of the central source relates to its radio output (e.g., Willott et al. 1999; De Breuck et al. 2000b).

While Table 3 shows that there is a possible correlation between L_{850} and $L_{3\text{GHz}}$ over the entire redshift range of our sample, this is probably an effect of the strong redshift dependence of both L_{850} and $L_{3\text{GHz}}$. The tests represented in Table 4 only take radio galaxies with $z > 2.5$ into account and even though this subsample contains almost all submm detections the correlation disappears. The scatterplot in Figure 5 is a graphical representation of the same result. We don’t find evidence for dust heating by AGN, in accordance with earlier findings (e.g., A01; Willott et al. 2002; Andreani et al. 2002) but see Haas et al. (2003) for a contrasting view based on ISO observations of local (most have $0.1 < z < 1.0$) hyperluminous quasars. This analysis is likely to be an oversimplification because the typical time-scales for starburst and radio activity differ by an order of magnitude.

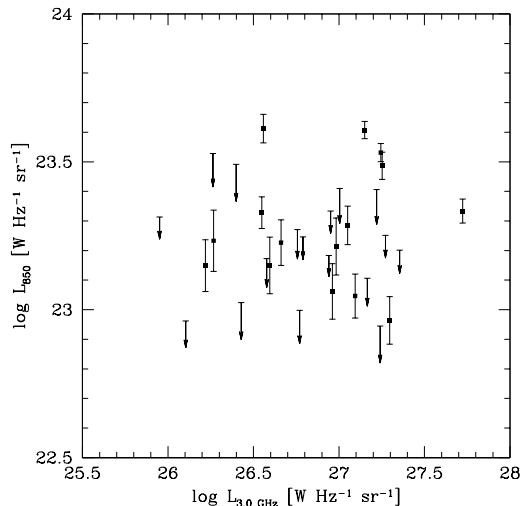


Figure 5. Submillimetre luminosity against radio power $L_{3\text{GHz}}$ for 32 radio galaxies with $z > 2.5$. No strong correlation is apparent, indicating that heating of the dust by AGN is not a dominant process for radio galaxies. Symbols as in Figure 1.

5.3 An anti-correlation between submm flux and UV polarisation

Optical polarimetry studies can be used to search for direct signs of starburst activity and determine the relative contributions of AGN and starburst to the UV continuum (e.g., Dey et al. 1997; Vernet et al. 2001). If the starburst dominates the UV/optical light, then the scattered (i.e. polarized) AGN light is diluted and one expects a low polarisation fraction of the UV continuum and perhaps a correlation with the observed submm flux densities.

Polarimetry results exist for 13 of the galaxies in our sample (Dey et al. 1997; Vernet et al. 2001, De Breuck et al. in preparation). A summary of the polarisation fractions and corresponding 850 μm flux densities is given in Table 5. We have plotted the observed submm flux density against UV continuum polarisation fraction in Figure 6. No sources with high UV polarisation are detected in the submm. This is supported formally by survival analysis: Kendall Tau gives a probability $P = 3$ per cent that there is no correlation.

This result is consistent with the view that for HzRGs star formation and submm emission are closely linked while any AGN contribution to the FIR is negligible. Tadhunter et al. (2002) also found some evidence for this. Two out of the three objects which are starburst dominated in their sample of 2-Jy radio galaxies are also extremely FIR luminous. Further support for low polarisation in starbursting systems comes from the luminous submm source SMM J02399–0136 (Vernet & Cimatti 2001) which shows only moderate ($P \sim 5$ per cent) polarisation.

The weakness of the submm luminosity in highly polarized sources together with the tentative correlation between $\text{Ly}\alpha$ and submm flux (see next section) is consistent with the anti-correlation between $\text{Ly}\alpha$ luminosity and UV polarisation reported by Vernet et al. (2001). They argue that $\text{Ly}\alpha$ photons are resonantly destructed by dust and that scattering by the same dust results in a higher fractional polarisation. This explanation, however, seems at odds with

Table 5. UV/optical polarisation fractions and submm fluxes for all radio galaxies for which both have been observed. UV/optical polarisation data are taken from Dey et al. (1997), Vernet et al. (2001), and De Breuck et al. in preparation, the submm data are from A01 and this paper.

Source	z	P(%)	S_{850} (mJy)
3C356	1.079	14	< 4.8
3C368	1.132	< 1	4.1
3C324	1.206	12	< 4.4
4C40.36	2.265	7.3	< 3.9
4C48.48	2.343	8.4	5.1
4C23.56	2.483	15.3	< 4.7
MRC0316–257	3.130	< 4	< 8.9
TNJ0121+1320	3.516	7	7.5
TX1243+036	3.570	11.3	< 5.6
6C1908+722	3.532	< 5	10.8
4C41.17	3.798	< 2.4	12.1
TNJ2007–1316	3.830	< 3	5.8
TNJ1338–1942	4.100	5	6.9

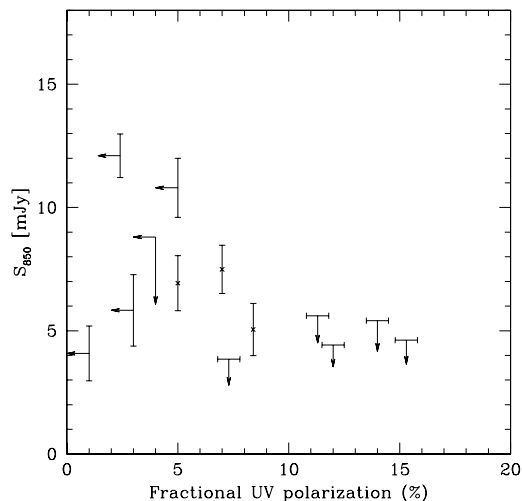


Figure 6. 850 μm flux S_{850} against observed UV continuum polarisation fraction. None of the highly polarized sources are detected in the submm, indicating that low polarisation (indicative of a starburst) and high L_{FIR} both trace star formation.

the lower submm flux densities in highly polarized sources unless there would be significant amounts of dust that is too hot to be detected in the submm.

5.4 Submillimetre and Ly α flux

Since many HzRGs are embedded in giant Ly α haloes (e.g., McCarthy 1993; van Ojik et al. 1996; Reuland et al. 2003) it would be interesting to see if one can relate the amount of available star formation ‘fuel’, as estimated roughly by the spatial size, or luminosity, of these emission line haloes and the amount of HI as probed by Ly α absorption to the observed rest-frame FIR luminosities. Alternatively, one might expect a strong anti-correlation due to destruction of Ly α emission by dust.

Many HzRGs are identified based on their Ly α line

and good data on the observed Ly α fluxes is available in most cases. There is a strong selection effect, however, since sources with low Ly α flux densities are less likely to be recognized as HzRGs. Interestingly, Table 4 and Figure 7 indicate that a correlation may be present. While this relation is tentative only, it offers perspectives for future programs. Better data should make it possible to investigate whether there is a possible relationship between the dust content and Ly α to C IV or NV emission line ratio, as indicators of metallicity (c.f. Vernet et al. 2001). This would be especially interesting in the light of findings by Hamann & Ferland (1999) and Fan et al. (2001) that QSOs show (super)solar abundances out to the highest redshifts and must already have undergone significant star formation. A comparison with the more readily studied HzRG host galaxies would be crucial to better understand this result.

The detection of both Ly α and dust in many HzRGs is intriguing because already a small amount of dust can extinguish Ly α radiation efficiently. The detection of Ly α in the submm sources of Chapman et al. (2003) is equally surprising. One explanation may be that Ly α emission and dust are located predominantly in different locations (e.g., a merger between one dusty and one less dusty component). Some evidence for this comes from 4C 60.07 at $z = 3.8$ in which the spatially resolved dust continuum emission (Papadopoulos et al. 2000) is anti-correlated with the Ly α emission (Fig. 5 in Reuland et al. 2003). Smail et al. (2003) also report evidence for an offset between far-IR and UV emitting regions in the $z = 2.38$ starburst galaxy N2 850.4.

5.5 L_{850} and linear size

Willott et al. (2002) found an anti-correlation between linear size and 850 μm luminosity for their sample of $z \sim 1.5$ radio loud quasars. This effect was attributed to a possible relation between the jet-triggering event and a short-lived starburst or quasar-heated dust in QSOs. No such correlation was found for a matched subset of the A01 sample centered at the same redshift. We have briefly investigated whether such a correlation exists in the present sample. Figure 8 shows the observed submm flux plotted against the projected linear size. No correction for possible differences in inclination angle was made because such corrections are expected to be relatively small among radio galaxies (even when comparing radio galaxies with quasars projection effects result in only a factor ≈ 1.6 difference in projected linear size for $\theta_{\text{trans}} = 53^\circ$; Willott et al. 2000, 2002). Our analysis does not support such a strong relation and if one interprets linear size as an estimate of the age of the radio source (reasonable if one assumes that the environments and jet powers do not change significantly; see e.g., Blundell et al. 1999), then this would be consistent with the scenario sketched by Willott et al. that the correlation found for QSOs is indicative of short starbursts while the starbursts in HzRGs have longer time-scales and could be forming the bulk of the stellar populations. Despite the absence of a clear correlation, some relation between age of radio source and starburst might have been expected if the black-hole and stellar bulge grow in a symbiotic fashion (e.g., Williams et al. 1999). However, in realistic scenarios many complicating factors can be envisaged such as the significantly different time-scales involved.

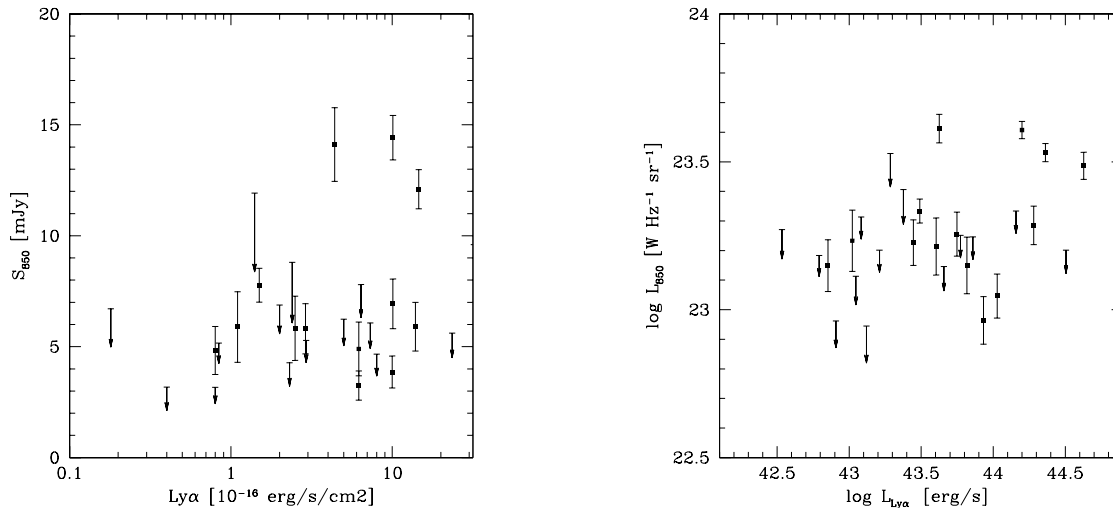


Figure 7. $S_{850\ \mu\text{m}}$ against observed $\text{Ly}\alpha$ line flux (left) and inferred luminosities L_{850} against $L_{\text{Ly}\alpha}$ (right). Tentative evidence for a correlation is apparent. The galaxies brightest in $\text{Ly}\alpha$ seem to have higher submm flux densities, possibly indicating that galaxies with richer gaseous environments (as traced by $\text{Ly}\alpha$) also host more massive starbursts. Symbols as in Figure 1.

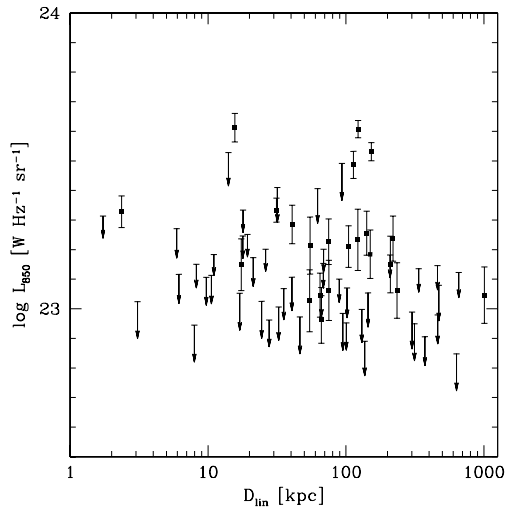


Figure 8. 850 μm luminosity L_{850} against the radio source projected linear size D_{lin} . There is no evidence for a strong anti-correlation as was found for radio loud quasars by Willott et al. (2002). Symbols as in Figure 1.

Growth of the radio source may first induce star formation by compressing molecular clouds (Begelman & Cioffi 1989; Bicknell et al. 2000) and may then actually signal the end of the starburst by clearing out all the cool gas from the central region (Rawlings 2003).

5.6 Submillimetre and near-IR emission

As discussed by Isaak et al. (2002), for QSOs one might naively expect a correlation between the submm and optical flux densities. This correlation might arise regardless of whether stars or a buried AGN are responsible for heating of the dust since black hole mass scales with stellar bulge mass. Priddey et al. (2003) note that the picture is likely to

be more complex and that any correlation might be smeared out due to differences in relative timing between AGN fueling and starburst, or varying dust-torus geometries. Radio galaxies might be better suited for such studies, since according to orientation based unification schemes (e.g., Barthel 1989) the AGN are obscured by a natural coronagraph and rest-frame B -band luminosity therefore is a fairly reliable measure of the mass of the stellar population or starburst activity. For this reason we have correlated the K -band magnitudes (samples rest-frame B, V for $z > 3$) with the submm flux densities. As can be seen from Table 4 and Figure 9 no such correlation is apparent. This remains true, if we apply a K -correction to the near-IR magnitudes. However, the dataset is rather inhomogeneous and more sensitive data in both the submm and near-IR are required to truly rule out any correlation. Sensitive multi-band observations could be used to (i) construct a redshift independent estimate of the line-free rest-frame optical continuum for comparison with L_{FIR} ([O III] and $\text{H}\alpha$ can sometimes dominate the K -band e.g., 4C 30.36, 4C 39.37; Egami et al. 2003), and (ii) check whether FIR emission is stronger for sources with higher intrinsic reddening (following e.g., Calzetti 1997; Adelberger & Steidel 2000; Seibert et al. 2002).

5.7 Summary

From our analysis we consider the following results the most interesting:

- (i) S_{850} and z are strongly correlated. Whether this is true also for L_{FIR} and z depends on the assumed dust template.
- (ii) L_{850} and radio power $L_{3\text{GHz}}$ do not correlate strongly, indicating that AGN do not dominate the submm emission (either through synchrotron contamination or dust heating by the UV continuum).
- (iii) S_{850} and $\text{Ly}\alpha$ appear weakly correlated. While this is not very convincing, the interesting result is the absence of a strong anti-correlation as expected naively from the destruction of $\text{Ly}\alpha$ emission by dust.

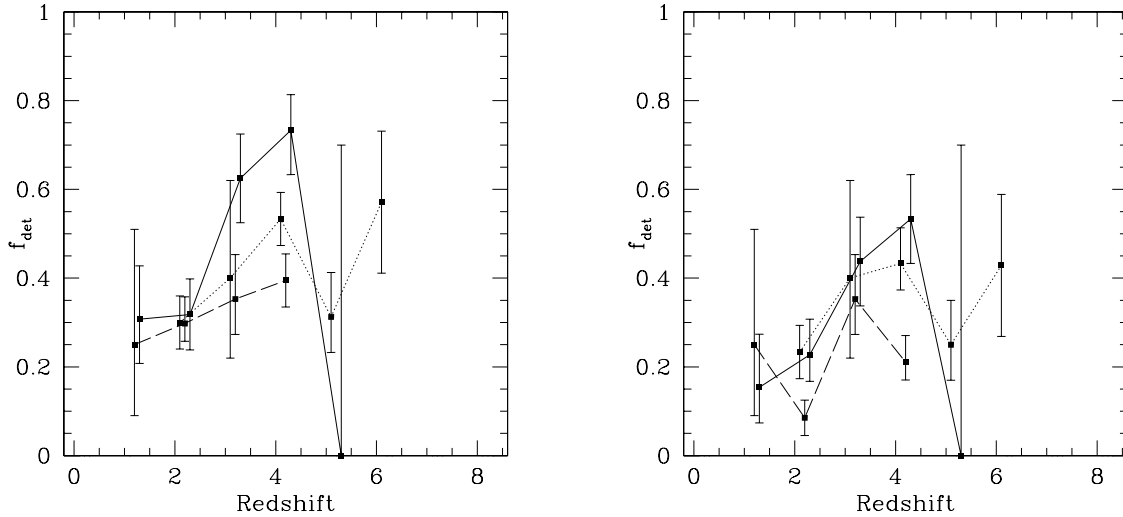


Figure 10. The $850\ \mu\text{m}$ detection (left $S/N > 2$; right $S/N > 3$) fractions of radio galaxies as function of redshift (solid line). The fractions rise up to a redshift of $z = 4$. For comparison we also plot the detection fraction for observations of radio quiet QSOs at $z = 1 - 5$, and radio loud quasars at $z \sim 1.5$ (after matching the sensitivity to $3\ \text{mJy rms}$) at $850\ \mu\text{m}$ (dashed line; Priddey et al. 2003; Isaak et al. 2002; Willott et al. 2002) and $1.25\ \text{mm}$ (dotted line; Omont et al. 2001, 2003; Carilli et al. 2001; Petric et al. 2003; Bertoldi et al. 2003). The detection rates for the QSOs appear to follow the same trend as for the radio galaxies, but the QSO datapoint at $z = 5$ seems indicative of a turnover (the $z = 5$ point for the HzRGs is based on only 1 galaxy, but taking all $z > 4$ HzRGs yields a similar result). The datapoint at $z = 6$ could indicate a detection fraction larger even than what is observed for $z = 4$. This might reflect, the extreme properties of those sources.

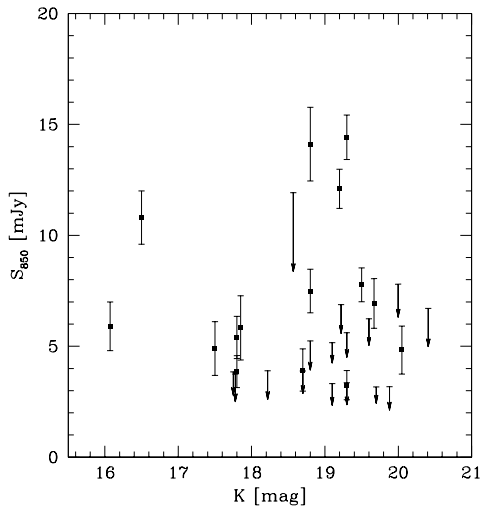


Figure 9. $S_{850\ \mu\text{m}}$ against observed K -band magnitude. No correlation is apparent, and no relation between L_{FIR} and stellar mass/optical star formation rate of the host galaxy can be established. Symbols as in Figure 1.

(iv) S_{850} and UV polarisation fraction appear anti-correlated. This is expected if the UV continuum of the buried AGN does not contribute significantly to the dust heating.

6 A COMPARISON OF RADIO GALAXIES WITH QSOS

The optically thin (sub-)mm emission of starbursts should be largely independent of viewing angle. Orientation based unification schemes for AGN (e.g., Barthel 1989) therefore suggest that we can combine observations of radio galaxies with those of QSOs, allowing us to study the evolution of star formation in their host galaxies over a larger redshift range. Extensive surveys of high-redshift (mostly radio-quiet) QSOs have been published recently (Carilli et al. 2001; Omont et al. 2001, 2003; Isaak et al. 2002; Priddey et al. 2003; Petric et al. 2003; Bertoldi et al. 2003). We have combined their results and compare those with our sample.

Figure 10 shows the detection fraction as a function of redshift for the QSO and radio galaxy samples. In many redshift bins only a small number of detections and non-detections is responsible for estimating the success rates for the present effective flux limits. We have estimated the range over which the ‘true success rate’ could vary such that there would be a 68 per cent chance of measuring the observed detection fraction. This range is indicated by the errorbars. Figure 11 shows the average (sub-)mm flux density for the various samples as a function of redshift.

Reassuringly, the trends for the QSOs and radio galaxies shown in these figures mimic each other. The average observed (sub-)mm flux density rises to redshifts of $z \sim 4$. For higher redshifts there is some evidence for a decline (see the discussion in Section 5.1.3 and the $z = 5$ data point of the MAMBO QSO observations). However, the observations of $z > 4$ QSOs would also be consistent with a fairly constant or even a rise in the detection fraction and average FIR luminosity out to the highest redshifts. This depends

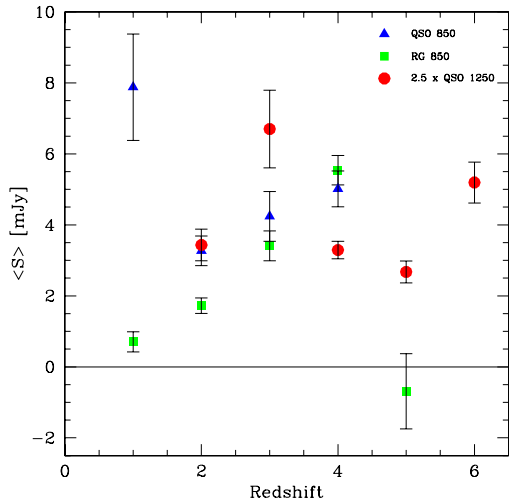


Figure 11. The average measured (sub-)mm flux density binned in redshift has been plotted for QSOs and radio galaxies. The squares represent observations of radio galaxies at 850 μm , the triangles QSOs at 850 μm , while the circles represent observations of QSOs at 1250 μm multiplied by a factor of 2.5 for easier comparison. The datapoint at $z \approx 1.5$ represents the radio loud quasars from Willott et al. (2002). The trends with redshift are similar to what is seen in Figure 10 and confirm the steady rise from $z = 1$ to $z = 4$ for the galaxies.

rather critically on the $z \sim 6$ QSOs, which are likely to be atypical even for QSOs.

The average flux density and detection rate of the QSOs is comparable to that of the HzRGs, even though the HzRG surveys are more sensitive than the QSO surveys by a factor of approximately 3. This, coupled with the assumption that quasars are on average more luminous than radio galaxies in AGN unification schemes based on receding torus models (e.g., Simpson 2003), may be viewed as further support for an AGN related component in QSOs, similar to what was found for radio quasars (Andreani et al. 2002; Willott et al. 2002). Note that the quasars discussed by Willott et al. (2002) are exceptionally bright compared to the mostly radio quiet QSOs represented in Figs. 10,11.

Due to a lack of carefully matched surveys fundamental differences between type I and type II AGN and radio-loud versus radio-quiet targets cannot be properly investigated yet, although slowly progress is being made.

7 SUMMARY

We have presented SCUBA observations of 24 radio galaxies and compared those with earlier results of 47 radio galaxies from the survey by A01. We confirm that HzRGs are massive forming galaxies, forming stars up to rates of a few thousand $M_{\odot} \text{yr}^{-1}$ and that there is no strong evidence for a correlation with radio power. Further evidence for a predominantly starburst nature of the far-IR emission comes from the striking anti-correlation between submm flux density and UV polarisation (Fig. 6).

In agreement with A01 we find that submm detection rate appears to be primarily a function of redshift. If this is

interpreted as being due to a change in the intrinsic far-IR luminosity, it would be consistent with a scenario in which the bulk of the stellar population of radio galaxies forms rapidly around redshifts of $z = 3 - 5$ after which they are more passively evolving (c.f. Best et al. 1998). We also find that the median redshift of the HzRGs with SCUBA detections ($z = 3.1$) is higher than the median redshift of the submm population ($z = 2.4$; Chapman et al. 2003). In the current picture of hierarchical galaxy formation, this could be interpreted as that HzRGs are more massive galaxies, which are then thought to begin their collapse at earlier cosmic times and evolve faster and finish the bulk of their formation process earlier. Alternatively, it could indicate that higher redshift submm sources are being missed due to the requirement of a radio counterpart prior to spectroscopic follow-up.

HzRGs have accurately determined redshifts and host identifications and are thought to be the most massive galaxies at any epoch (De Breuck et al. 2002). Therefore, HzRGs are a key population for studies of galaxy formation in the early universe, allowing detailed follow-up mm-interferometry observations to study their dust and gas content. Currently, they offer the best way to obtain reliable dynamic masses for a significant number of massive high redshift galaxies. These HzRGs would be especially suited to constrain any evolution in galaxy mass with redshift, study changes in evolutionary status, gas mass, and the starburst-AGN connection. If all of these turn out to have masses larger than $10^{11} M_{\odot}$, then this could have important consequences (depending on rather uncertain correction factors for the fraction of similar galaxies for which the black hole is dormant) for our understanding of galaxy formation, because only few such massive galaxies are expected at such high redshifts (Genzel et al. 2003).

ACKNOWLEDGMENTS

We thank Chris Willott and Steve Rawlings for useful discussions and the anonymous referee for helpful suggestions to improve the paper. We gratefully acknowledge the excellent help of the JCMT staff and ‘flexible’ observers who collected data for our program. In particular the help of Remo Tilanus was indispensable. The authors wish to extend special thanks to those of Hawaiian ancestry on whose sacred mountain we are privileged to be guests. The JCMT is operated by JAC, Hilo, on behalf of the parent organizations of the Particle Physics and Astronomy Research Council in the UK, the National Research Council in Canada and the Scientific Research Organization of the Netherlands. The work of M.R. and W.v.B. was performed under the auspices of the U.S. Department of Energy, National Nuclear Security Administration by the University of California, Lawrence Livermore National Laboratory under contract No. W-7405-Eng-48.

REFERENCES

- Adelberger K. L., Steidel C. C., 2000, ApJ, 544, 218
- Andreani P., Fosbury R. A. E., van Bemmell I., Freudling W., 2002, A&A, 381, 389

- Archibald E. N., Dunlop J. S., Hughes D. H., Rawlings S., Eales S. A., Ivison R. J., 2001, *MNRAS*, 323, 417
- Archibald E. N., Jenness T., Holland W. S., Coulson I. M., Jessop N. E., Stevens J. A., Robson E. I., Tilanus R. P. J., Duncan W. D., Lightfoot J. F., 2002, *MNRAS*, 336, 1
- Aretxaga I., Hughes D. H., Chapin E. L., Gaztañaga E., Dunlop J. S., Ivison R. J., 2003, *MNRAS*, 342, 759
- Athreya R. M., Kapahi V. K., McCarthy P. J., van Breugel W., 1997, *MNRAS*, 289, 525
- Barthel P. D., 1989, *ApJ*, 336, 606
- Begelman M. C., Cioffi D. F., 1989, *ApJ*, 345, L21
- Bertoldi F., Carilli C. L., Cox P., Fan X., Strauss M. A., Beelen A., Omont A., Zylka R., 2003, *A&A*, 406, L55
- Bertoldi F., Menten K. M., Kreysa E., Carilli C. L., Owen F., 2002, *Highlights in Astronomy*, 12, 473
- Best P. N., Longair M. S., Röttgering H. J. A., 1998, *MNRAS*, 295, 549
- Bicknell G. V., Sutherland R. S., van Breugel W. J. M., Dopita M. A., Dey A., Miley G. K., 2000, *ApJ*, 540, 678
- Blain A. W., Smail I., Ivison R. J., Kneib J.-P., 1999, *MNRAS*, 302, 632
- Blundell K. M., Rawlings S., Willott C. J., 1999, *AJ*, 117, 677
- Calzetti D., 1997, *AJ*, 113, 162
- Carilli C. L., Bertoldi F., Rupen M. P., Fan X., Strauss M. A., Menten K. M., Kreysa E., Schneider D. P., Bertarini A., Yun M. S., Zylka R., 2001, *ApJ*, 555, 625
- Carilli C. L., Harris D. E., Pentericci L., Röttgering H. J. A., Miley G. K., Kurk J. D., van Breugel W., 2002, *ApJ*, 567, 781
- Chapman S. C., Blain A. W., Ivison R. J., Smail I. R., 2003, *Nature*, 422, 695
- Chapman S. C., Scott D., Borys C., Fahlman G. G., 2002a, *MNRAS*, 330, 92
- Chapman S. C., Shapley A., Steidel C., Windhorst R., 2002c, *ApJ*, 572, L1
- Chapman S. C., Smail I., Ivison R. J., Blain A. W., 2002b, *MNRAS*, 335, L17
- Chini R., Kruegel E., Kreysa E., 1986, *A&A*, 167, 315
- Condon J. J., Cotton W. D., Greisen E. W., Yin Q. F., Perley R. A., Taylor G. B., Broderick J. J., 1998, *AJ*, 115, 1693
- Cowie L. L., Barger A. J., Kneib J.-P., 2002, *AJ*, 123, 2197
- De Breuck C., Neri R., Morganti R., Omont A., Rocca-Volmerange B., Stern D., Reuland M., van Breugel W., Röttgering H., Stanford S. A., Spinrad H., Vigotti M., Wright M., 2003, *A&A*, 401, 911
- De Breuck C., Röttgering H., Miley G., van Breugel W., Best P., 2000b, *A&A*, 362, 519
- De Breuck C., van Breugel W., Minniti D., Miley G., Röttgering H., Stanford S. A., Carilli C., 1999, *A&A*, 352, L51
- De Breuck C., van Breugel W., Röttgering H., Stern D., Miley G., de Vries W., Stanford S. A., Kurk J., Overzier R., 2001, *AJ*, 121, 1241
- De Breuck C., van Breugel W., Röttgering H. J. A., Miley G., 2000a, *A&AS*, 143, 303
- De Breuck C., van Breugel W., Stanford S. A., Röttgering H., Miley G., Stern D., 2002, *AJ*, 123, 637
- Dey A., 1999, in *The Most Distant Radio Galaxies The Early History of Powerful Radio Galaxies*. pp 19–+
- Dey A., Graham J. R., Ivison R. J., Smail I., Wright G. S., Liu M. C., 1999, *ApJ*, 519, 610
- Dey A., van Breugel W., Vacca W. D., Antonucci R., 1997, *ApJ*, 490, 698
- Douglas J. N., Bash F. N., Bozayan F. A., Torrence G. W., Wolfe C., 1996, *AJ*, 111, 1945
- Downes D., Radford J. E., Greve A., Thum C., Solomon P. M., Wink J. E., 1992, *ApJ*, 398, L25
- Drinkwater M. J., Webster R. L., Francis P. J., Condon J. J., Ellison S. L., Jauncey D. L., Lovell J., Peterson B. A., Savage A., 1997, *MNRAS*, 284, 85
- Dunlop J. S., McLure R. J., Kukula M. J., Baum S. A., O’Dea C. P., Hughes D. H., 2003, *MNRAS*, 340, 1095
- Dunlop J. S., McLure R. J., Yamada T., Kajisawa M., Peacock J. A., Mann R. G., Hughes D. H., Aretxaga I., Muxlow T. W. B., Richards A. M., Dickinson M., Ivison R. J., Smith G. P., Smail I., Serjeant S., Almaini O., Lawrence A., 2002, *ArXiv Astrophysics e-prints*
- Dunne L., Eales S., Edmunds M., Ivison R., Alexander P., Clements D. L., 2000, *MNRAS*, 315, 115
- Dunne L., Eales S., Ivison R., Morgan H., Edmunds M., 2003, *Nature*, 424, 285
- Dunne L., Eales S. A., 2001, *MNRAS*, 327, 697
- Dupac X., Bernard J.-P., Boudet N., Giard M., Lamarre J.-M., Mény C., Pajot F., Ristorcelli I., Serra G., Stepnik B., Torre J.-P., 2003, *A&A*, 404, L11
- Eales S., Bertoldi F., Ivison R., Carilli C., Dunne L., Owen F., 2003, *MNRAS*, 344, 169
- Eales S., Lilly S., Webb T., Dunne L., Gear W., Clements D., Yun M., 2000, *AJ*, 120, 2244
- Eales S. A., Rawlings S., 1996, *ApJ*, 460, 68
- Edmunds M. G., 2001, *MNRAS*, 328, 223
- Egami E., Armus L., Neugebauer G., Murphy T. W., Soifer B. T., Matthews K., Evans A. S., 2003, *AJ*, 125, 1038
- Fan X., Narayanan V. K., Lupton R. H., Strauss M. A., Knapp G. R., Becker R. H., White R. L., Pentericci L., Leggett S. K., Haiman Z., Gunn J. E., Ivezić Ž., Schneider D. P., Anderson S. F., Brinkmann J., 2001, *AJ*, 122, 2833
- Farrah D., Serjeant S., Efstathiou A., Rowan-Robinson M., Verma A., 2002, *MNRAS*, 335, 1163
- Feigelson E. D., Nelson P. I., 1985, *ApJ*, 293, 192
- Frayser D. T., Armus L., Scoville N. Z., Blain A. W., Reddy N. A., Ivison R. J., Smail I., 2003, *AJ*, 126, 73
- Frayser D. T., Reddy N. A., Armus L., Blain A. W., Scoville N. Z., Smail I., 2004, *AJ*, 127, 728
- Genzel R., Baker A. J., Tacconi L. J., Lutz D., Cox P., Guilloteau S., Omont A., 2003, *ApJ*, 584, 633
- Haas M., Klaas U., Müller S. A. H., Bertoldi F., Camenzind M., Chini R., Krause O., Lemke D., Meisenheimer K., Richards P. J., Wilkes B. J., 2003, *A&A*, 402, 87
- Hamann F., Ferland G., 1999, *ARA&A*, 37, 487
- Hogg D. W., 2001, *AJ*, 121, 1207
- Holland W. S., Robson E. I., Gear W. K., Cunningham C. R., Lightfoot J. F., Jenness T., Ivison R. J., Stevens J. A., Ade P. A. R., Griffin M. J., Duncan W. D., Murphy J. A., Naylor D. A., 1999, *MNRAS*, 303, 659
- Hughes D. H., Dunlop J. S., Rawlings S., 1997, *MNRAS*, 289, 766
- Hughes D. H., Serjeant S., Dunlop J., Rowan-Robinson M., Blain A., Mann R. G., Ivison R., Peacock J., Efstathiou A., Gear W., Oliver S., Lawrence A., Longair M., Goldschmidt P., Jenness T., 1998, *Nature*, 394, 241
- Isaak K. G., Priddey R. S., McMahon R. G., Omont A.,

- Peroux C., Sharp R. G., Withington S., 2002, MNRAS, 329, 149
- Isobe T., Feigelson E. D., Nelson P. I., 1986, ApJ, 306, 490
- Ivison R. J., Dunlop J. S., Smail I., Dey A., Liu M. C., Graham J. R., 2000, ApJ, 542, 27
- Ivison R. J., Smail I., Le Borgne J.-F., Blain A. W., Kneib J.-P., Bezecourt J., Kerr T. H., Davies J. K., 1998, MNRAS, 298, 583
- James A., Dunne L., Eales S., Edmunds M. G., 2002, MNRAS, 335, 753
- Jenness T., Lightfoot J. F., 1998, in ASP Conf. Ser. 145: Astronomical Data Analysis Software and Systems VII Reducing SCUBA Data at the James Clerk Maxwell Telescope. pp 216–+
- Jenness T., Stevens J. A., Archibald E. N., Economou F., Jessop N., Robson E. I., Tilanus R. P. J., Holland W. S., 2001, in ASP Conf. Ser. 238: Astronomical Data Analysis Software and Systems X Automated Reduction and Calibration of SCUBA Archive Data Using ORAC-DR. pp 299–+
- Kapahi V. K., Athreya R. M., van Breugel W., McCarthy P. J., Subrahmanya C. R., 1998, ApJ, 118, 275
- Lacy M., 1999, in The Most Distant Radio Galaxies Galaxies and clusters around and in front of radio sources at $0.5 < z < 4.5$. pp 437–+
- Lacy M., Laurent-Muehleisen S. A., Ridgway S. E., Becker R. H., White R. L., 2001, ApJ, 551, L17
- Lavalley M., Isobe T., Feigelson E., 1992, in ASP Conf. Ser. 25: Astronomical Data Analysis Software and Systems I ASURV: Astronomy Survival Analysis Package. pp 245–+
- Ledlow M. J., Smail I., Owen F. N., Keel W. C., Ivison R. J., Morrison G. E., 2002, ApJ, 577, L79
- McCarthy P. J., 1993, ARA&A, 31, 639
- McCarthy P. J., Kapahi V. K., van Breugel W., Persson S. E., Athreya R., Subrahmanya C. R., 1996, ApJ, 107, 19
- McCarthy P. J., Kapahi V. K., van Breugel W., Subrahmanya C. R., 1990, AJ, 100, 1014
- Omont A., Beelen A., Bertoldi F., Cox P., Carilli C. L., Priddey R. S., McMahon R. G., Isaak K. G., 2003, A&A, 398, 857
- Omont A., Cox P., Bertoldi F., McMahon R. G., Carilli C., Isaak K. G., 2001, A&A, 374, 371
- Ouchi M., Shimasaku K., Okamura S., Doi M., Furusawa H., Hamabe M., Kimura M., Komiyama Y., Miyazaki M., Miyazaki S., Nakata F., Sekiguchi M., Yagi M., Yasuda N., 2001, ApJ, 558, L83
- Papadopoulos P. P., Röttgering H. J. A., van der Werf P. P., Guilloateau S., Omont A., van Breugel W. J. M., Tilanus R. P. J., 2000, ApJ, 528, 626
- Pentericci L., Röttgering H. J. A., Miley G. K., McCarthy P., Spinrad H., van Breugel W. J. M., Macchetto F., 1999, A&A, 341, 329
- Pentericci L., Röttgering H. J. A., Miley G. K., Carilli C. L., McCarthy P., 1997, A&A, 326, 580
- Pentericci L., Röttgering H. J. A., Miley G. K., Spinrad H., McCarthy P. J., van Breugel W. J. M., Macchetto F., 1998, ApJ, 504, 139
- Petric A. O., Carilli C. L., Bertoldi F., Fan X., Cox P., Strauss M. A., Omont A., Schneider D. P., 2003, AJ, 126, 15
- Priddey R. S., Isaak K. G., McMahon R. G., Omont A., 2003, MNRAS, 339, 1183
- Priddey R. S., McMahon R. G., 2001, MNRAS, 324, L17
- Rawlings S., 2003, New Astronomy Review, 47, 397
- Rengelink R., 1998, Ph.D. Thesis
- Rengelink R. B., Tang Y., de Bruyn A. G., Miley G. K., Bremer M. N., Röttgering H. J. A., Bremer M. A. R., 1997, A&AS, 124, 259
- Reuland M., van Breugel W., Röttgering H., de Vries W., Stanford S. A., Dey A., Lacy M., Bland-Hawthorn J., Dopita M., Miley G., 2003, ApJ, 592, 755
- Röttgering H. J. A., van Ojik R., Miley G. K., Chambers K. C., van Breugel W. J. M., de Koff S., 1997, A&A, 326, 505
- Rowan-Robinson M., 2000, MNRAS, 316, 885
- Sanders D. B., Mirabel I. F., 1996, ARA&A, 34, 749
- Sanders D. B., Phinney E. S., Neugebauer G., Soifer B. T., Matthews K., 1989, ApJ, 347, 29
- Scott S. E., Fox M. J., Dunlop J. S., Serjeant S., Peacock J. A., Ivison R. J., Oliver S., Mann R. G., Lawrence A., Efstathiou A., Rowan-Robinson M., Hughes D. H., Archibald E. N., Blain A., Longair M., 2002, MNRAS, 331, 817
- Seibert M., Heckman T. M., Meurer G. R., 2002, AJ, 124, 46
- Simpson C., 2003, New Astronomy Review, 47, 211
- Smail I., Chapman S. C., Ivison R. J., Blain A. W., Takata T., Heckman T. M., Dunlop J. S., Sekiguchi K., 2003, MNRAS, 342, 1185
- Smail I., Ivison R. J., Blain A. W., Kneib J.-P., 2002, MNRAS, 331, 495
- Sohn B. W., Klein U., Mack K.-H., 2003, A&A, 404, 133
- Soucail G., Kneib J. P., Bézecourt J., Metcalfe L., Altieri B., Le Borgne J. F., 1999, A&A, 343, L70
- Steidel C. C., Adelberger K. L., Giavalisco M., Dickinson M., Pettini M., 1999, ApJ, 519, 1
- Steidel C. C., Giavalisco M., Pettini M., Dickinson M., Adelberger K. L., 1996, ApJ, 462, L17+
- Stern D., Dey A., Spinrad H., Maxfield L., Dickinson M., Schlegel D., González R. A., 1999, AJ, 117, 1122
- Stevens J. A., Ivison R. J., Dunlop J. S., Smail I. R., Percival W. J., Hughes D. H., Röttgering H. J. A., van Breugel W. J. M., Reuland M., 2003, Nature, 425, 264
- Tadhunter C., Dickson R., Morganti R., Robinson T. G., Wills K., Villar-Martín M., Hughes M., 2002, MNRAS, 330, 977
- Tody D., 1993, in ASP Conf. Ser. 52: Astronomical Data Analysis Software and Systems II IRAF in the Nineties. pp 173–+
- van Breugel W., De Breuck C., Stanford S. A., Stern D., Röttgering H., Miley G., 1999, ApJ, 518, L61
- van Ojik R., Röttgering H. J. A., Carilli C. L., Miley G. K., Bremer M. N., Macchetto F., 1996, A&A, 313, 25
- van Ojik R., Röttgering H. J. A., Miley G. K., Hunstead R. W., 1997, A&A, 317, 358
- Venemans B. P., Kurk J. D., Miley G. K., Röttgering H. J. A., 2003, New Astronomy Review, 47, 353
- Vernet J., Cimatti A., 2001, A&A, 380, 409
- Vernet J., Fosbury R. A. E., Villar-Martín M., Cohen M. H., Cimatti A., di Serego Alighieri S., Goodrich R. W., 2001, A&A, 366, 7
- Waddington I., Windhorst R. A., Dunlop J. S., Koo D. C., Peacock J. A., 2000, MNRAS, 317, 801

- Webb T. M., Eales S., Foucaud S., Lilly S. J., McCracken H., Adelberger K., Steidel C., Shapley A., Clements D. L., Dunne L., Le Fèvre O., Brodwin M., Gear W., 2003b, *ApJ*, 582, 6
- Webb T. M., Eales S. A., Lilly S. J., Clements D. L., Dunne L., Gear W. K., Ivison R. J., Flores H., Yun M., 2003a, *ApJ*, 587, 41
- Williams R. J. R., Baker A. C., Perry J. J., 1999, *MNRAS*, 310, 913
- Willott C. J., Rawlings S., Archibald E. N., Dunlop J. S., 2002, *MNRAS*, 331, 435
- Willott C. J., Rawlings S., Blundell K. M., Lacy M., 1999, *MNRAS*, 309, 1017
- Willott C. J., Rawlings S., Blundell K. M., Lacy M., 2000, *MNRAS*, 316, 449

This paper has been typeset from a $\text{\TeX}/\text{\LaTeX}$ file prepared by the author.